Monitoring of Inflatable Structures by Using Virtual Image Correlation

Alexis Bloch, M.L.M. François, Jean-Christophe Thomas, Olivier Flamand

7th European Workshop on Structural Health Monitoring
July 8-11, 2014. La Cité, Nantes, France

MONITORING OF INFLATABLE STRUCTURES BY USING VIRTUAL IMAGE CORRELATION

Alexis Bloch[1], **Marc François**[1], **Jean-Christophe Thomas**[1], **Olivier Flamand**[2]

[1] *GeM, CNRS UMR 6183, Université de Nantes, 2 rue de la Houssinière, 44322 Nantes*
[2] *Centre Scientifique des Techniques du Bâtiment (CSTB), 11 rue Henri Picherit 44323 Nantes*

marc.francois@univ-nantes.fr

ABSTRACT

The VIC method consists in finding the analytical contour by fitting the boundary of the objet in the picture as best as possible. It has been used for shape measurement of an inflatable beam submitted to a transverse wind in the CSTB wind tunnel in Nantes. The principle and the main equations of the method are recalled. The originality of this study is that the equation of the contour is deduced from the analytical expression of the deformation of an inflatable beam under a distributed constant (aerodynamic) load. This acts as a powerful mechanical-based filter and leads straightforwardly to the researched mechanical properties of the textile membrane.

KEYWORDS : *Image correlation, inflatable structure, measurement, SHM*

INTRODUCTION

Due to their low cost, light weight and environmental performance, inflatable and tended fabric structures are increasingly used in Civil Engineering. They are highly deformable so they require adapted monitoring devices. The knowledge of the displacement field is crucial for the model validation and for the inflatable structures computation and certification. The magnitude of displacements and the structures sizes make the imaging methods to be nearly the only ones available.

The quite new Digital Image Correlation (DIC) methods [1] are contactless and applied for strain field measurement. However, they require a painted speckle and may difficultly deal with large displacement. The Virtual Image Correlation (VIC) method [2] (initially derived from the DIC) consists in finding the best correlation between the contour of the structure and a parameterized curve. A virtual image is created from the curve mathematical expression. The virtual image boundary presents a continuous evolution from black to white determined by the distance from the curve. The correlation is straightforwardly related to the curve parameters and the best one (the lowest distance between the physical image and the virtual one) corresponds to the superposition of the virtual image contour on the object boundary. The returned information is the analytical description of the contour (not a collection of pixels). Present version only allows to measure a plane displacement but a 3D extension is possible. The precision of the measurement in case of ideal images is sub-pixel (theoretically 1/1000 pixel [3]). The curve equation may be generic (circle, B-Splines...) or, as here, a solution to the mechanical problem (here an inflatable beam). In this case, the curve parameters include some non-dimensional terms such as a ratio between load and stiffness whose identification allows to recover the beam mechanical properties (stiffness since load is given by the aerodynamical data).

Experimentation consists in a transversally located inflatable beam in a wind tunnel. Fixations are realized thanks to four cables whose role is to apply retainment forces without any parasite force or moment. Results are shown to validate an inflatable beam model and evaluate the mechanical properties of the inflatable beam.

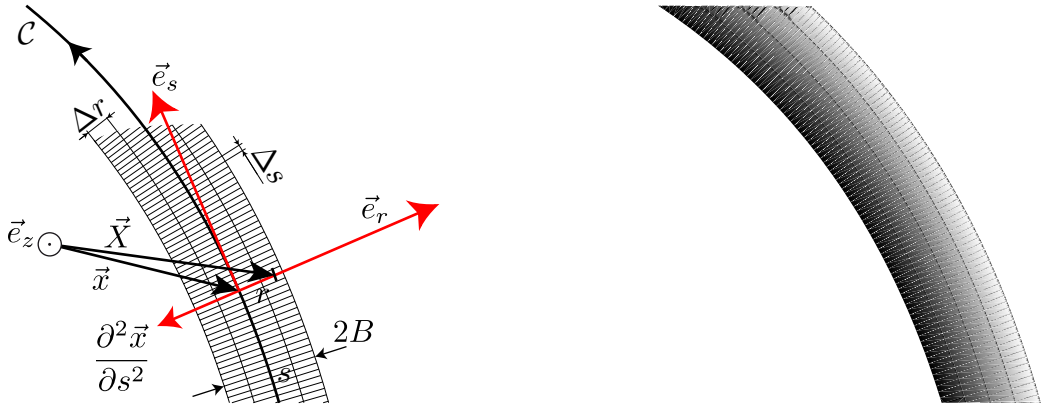

Figure 1 : a) left : the virtual image parameterization. b) right : the corresponding virtual image section

1. THE VIC METHOD

The virtual image is based on the analytical curve $\mathscr{C}$. It is computed as a fine mesh (typically three time finer than the pixel grid), in the curvilinear frame $\{\vec{e}_s, \vec{e}_r\}$, where the curvilinear abscissa s and the normal distance r are discretized respectively in Δr and Δs (see Figure 1a). The curve current point and the virtual beam corresponding one are defined respectively by vectors $\vec{x}$ and $\vec{X} = \vec{x} + r\vec{e}_r$. The width of the virtual beam is $2B$. Let us remark that the computation is only done for pixels of the image which are in correspondance to the virtual image; thus a very few part of the full image is concerned. This leads to rather brief computation times (in minutes, depending on the physical image size, the actual value of B and the precision level). The gray levels of the virtual image $g(r)$ is assumed to range linearly from white (1) to black (0), only depending upon the distance r from the curve. For the detection of a contour, this corresponds to:

$$g(r) = \frac{1}{2}\left(1 + \frac{r}{B}\right) \tag{1}$$

An example of such virtual image portion is given in Figure 1b. Of course, the boundary of the physical image is generally very different from this smooth transition from back to white. It might be sharper or it may contains some blurriness or presents a staircase aspect due to the pixel digitalization on neither vertical nor horizontal parts. However, the virtual image offers best correlation as soon as the virtual image mean line passes by the boundary of the physical object [3]. The distance Φ between the physical image F and the virtual one G is given by the quadratic distance φ divided by the surface of the virtual image S:

$$\varphi(V_k) = \iint_{\mathscr{D}_G} (F - G)^2 \, dS \tag{2}$$

$$\Phi(V_k) = \frac{\varphi(V_k)}{S(V_k)}, \tag{3}$$

Dividing by the distance avoids to minimize it; in other words it avoids line tension to appear which would lead to inaccurate correlation. The curve control parameters are denoted as the pseudo-vector V_k. For example, in case of a circle, the identification parameters are the two coordinates of the center and the radius. For a B-Spline, they are the control points coordinates. The minimization strategy consists in:

- Propose a starting guess thanks to a segment by segment detection procedure (or by any other contour detection method available).
- Compute the corresponding initial control parameters V_k and set a rather large width B
- Minimize the distance Φ thanks to a steepest slope method (the gradient $\partial\Phi/\partial V_k$ has an analytical or semi-analytical expression).
- Diminish the virtual image width B as soon as possible (when the contour of the physical image is fully embedded in the virtual image).
- Stop the procedure when Φ has decreased few enough between two successive iterations.

Various tests [3] show that the arbitrary width B has a weak influence on the precision of the identification. However, the less is B, the less is the computation time and a tiny width helps the virtual image not to see possible artifacts in the figure. Figure 3 shows the full procedure for an ideal disk detection thanks to a B-Spline (remind that a B-Spline cannot exactly describe a circle). This example shows that control points do not only move orthogonally to the contour but also tangentially in order to offer the best fit (the four points are quite regularly disposed at final state so the global error is minimised). Of course, the number of control points should be increased if sub-pixel precision is required. An

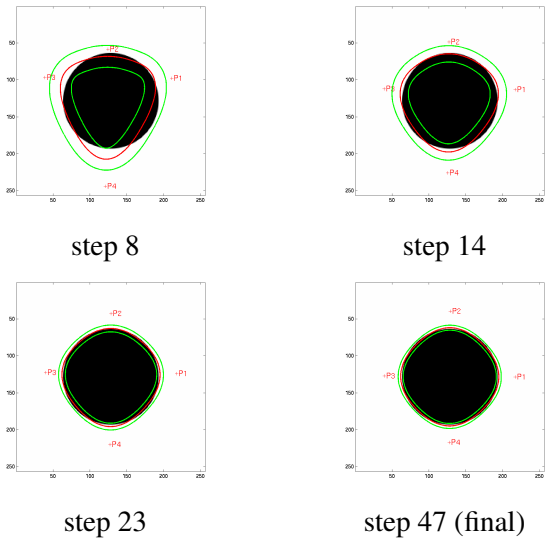

Figure 2 : Correlation process onto a circular disk by a 4-point B-Spline of order 2.

important information is contained in the physical image seen from the unwrapped curvilinear frame of the virtual image. If the correlation has succeeded, this picture should exhibit a continuous and regular (along the curvilinear abscissa) evolution from black to white. The sketch on Figure 3 clearly shows four waves corresponding to the lack of correlation between the four control points. The apparent blur is due to the interpolation of the physical image pixels (which is only 256×256 pixels in this case).

Figure 3 : Part of the physical image seen in the unwrapped frame of the virtual image.

2. THE EXPERIMENT

This test has been performed on a 4.5 m long and 0.27 m in diameter inflatable cylinder transversally disposed inside the CSTB wind tunnel. The "Ferrari F302" fabric is equilibrated and orthotropic. It is made of glass fiber and PVC matrix. A couple of objectives is set:

- Validate the simplified inflatable beam theory models.
- Validate the possibility of shape measurement by using VIC measurement presented above.

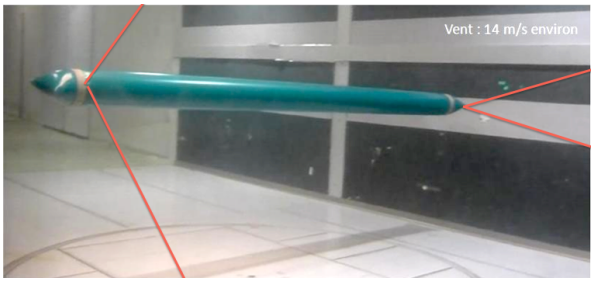

Figure 4 : The inflatable beam in the wind tunnel (average air velocity : 14 m/s). The four cables are colorized to highlight their location.

The beam is retained by two cables on each sides to ensure a pure bending trial. Figure 4 was captured by the control camera and is illustrative. A Kodak DCS camera (of better definition) is installed above the beam in the roof of the wind tunnel to perform VIC shape measurements.

3. THE SHAPE IDENTIFICATION WITH THE VIC METHOD

As mentioned in the introduction, the VIC method can use a curve equation issued from the mechanical problem. In the present case, it consists in a classical problem of a beam simply sustained at its ends (free ends rotations) and subjected to a distributed load due to aerodynamic effects. This hypothesis is validated by the controlled turbulence in the wind tunnel which leads to a quite uniform wind speed all along the beam (a gap of $\simeq 0.5$ m remains between the beam edges and the tunnel walls). Some resonance phenomena happened for particular wind speeds. These dynamic effects of great interest will be investigated in the future.

In this study, the results provided by both Euler-Bernoulli and Timoshenko beam theories are compared. In the second case, the in-plane displacement v of the mean line is expressed with respect to the abscissa $x \in [0, L]$ as:

$$v(x) = \frac{fL^2}{2(P+kGS)}\left(\left(\frac{x}{L}\right) - \left(\frac{x}{L}\right)^2\right) + \frac{fL^4}{24\left(E+\frac{P}{S}\right)I}\left(\left(\frac{x}{L}\right)^4 - 2\left(\frac{x}{L}\right)^3 + \left(\frac{x}{L}\right)\right) \tag{4}$$

where E and G are respectively the Young and the shear moduli, k is the reduced section coefficient ($k = 0,5$ in present case), S is the cross-section, I the second moment of area and $P = p\pi R^2$ defines the additive stiffness term P/S associated to a pressure effect [4]. For the Euler-Bernoulli theory, the displacement expression is reduced to the second member. The aerodynamical distributed load is:

$$f = \rho R C_x V^2 \tag{5}$$

where the drag coefficient C_x. For our range of wind speed $V \in [10, 30]$ m/s and considering the radius $R = 0.135$ m in air at 20°C, Reynolds numbers of magnitude $10^5 - 10^6$ are found (so C_x varies from 1 to 0.4).

The virtual image is based on the curve which corresponds to the deformed theoretical beam edge. This edge is constructed by using the beam theory: to any point of the mean line correspond two points (upper and lower) orientated along the actual direction of the beam cross-section. In the case of Euler-Bernoulli theory, the section is assumed to remain orthogonal to the mean line. In the case of Timoshenko theory, the rotation of the section for the current problem is given by:

$$\theta(x) = \frac{fL^3}{24\left(E+\frac{P}{S}\right)I}\left(4\left(\frac{x}{L}\right)^3 - 6\left(\frac{x}{L}\right)^2 + 1\right) \tag{6}$$

The optimization parameters V_k must be defined for the VIC method application. In the present problem, they are written as:

$$V_k = \left\{ \frac{fL^4}{\left(E+\frac{P}{S}\right)I}, \frac{fL^2}{P+kGS}, R, L, x_0, y_0, \theta_0 \right\} \tag{7}$$

The two first parameters are mechanical, the first is corresponding to the Euler-Bernoulli flexural

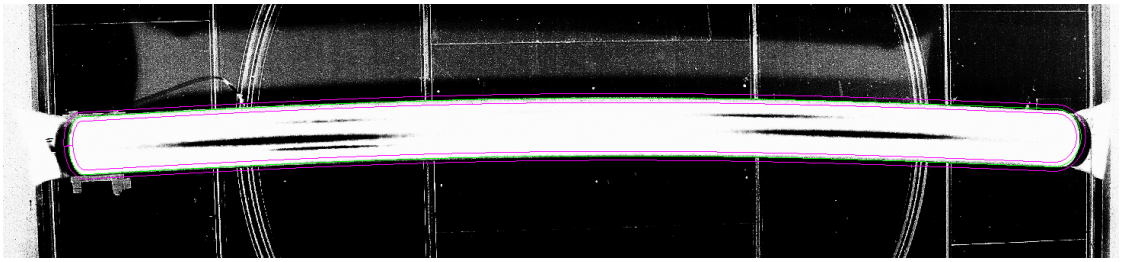

Figure 5 : Visualisation of the VIC method results under Bernoulli's hypothesis.

effects and the second is associated to the shear influence relating the Timoshenko theory. The next terms R and L are purely geometrical and the last ones correspond to the contour location (origin) and orientation in the frame of the image. All these parameters possesses the same dimension (m or pixel on photos) except for θ_0 and their magnitudes are close to each other (this make convergence easier).

Firstly, the computation does not take into account the (second) shear term (thus V_2 in Equation 7)

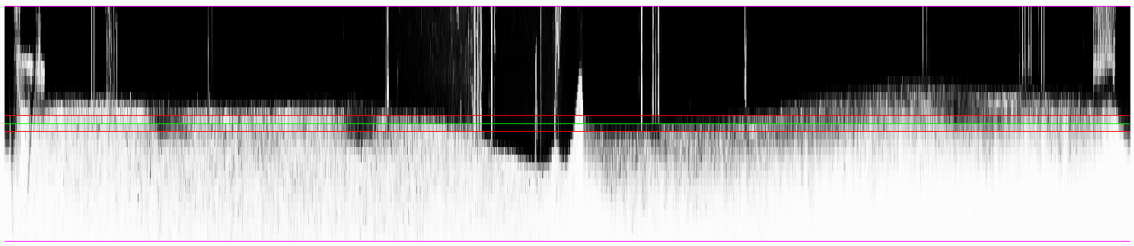

Figure 6 : Inflatable beam boundary seen in the unwrapped frame. The inner band shows the mean line and the pixel size.

and this corresponds to the Euler-Bernoulli hypothesis. The correlation between both virtual and real contour is shown by Figure 5 and by Figure 6 (of the same nature than Figure 3). A discrepancy between the best possible analytical shape and the physical contour can be noticed on Figure 6. Let us recall that the left half of the Figure 6 corresponds to the upper boundary; the very middle (where a peak is seen) corresponds to the right anchorage; the right part corresponds to the lower boundary.

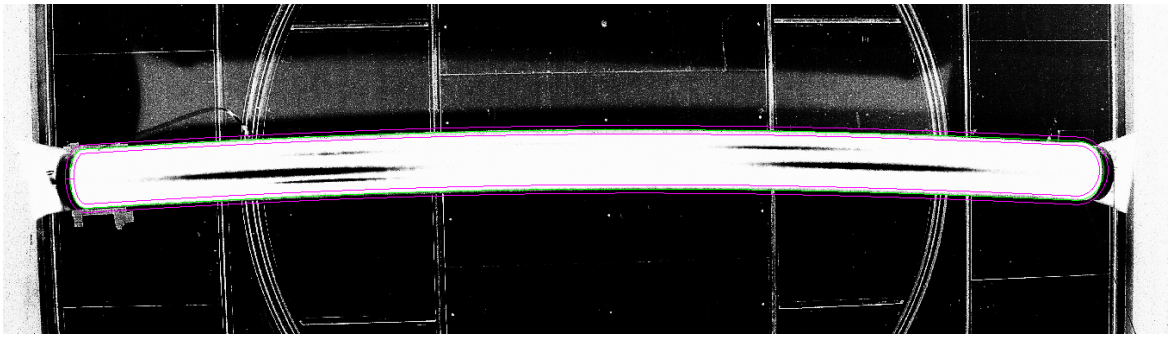

Figure 7 : Visualisation of the VIC method results under Timoshenko's hypothesis.

- The beam radius seems to be slightly wider on the left part than on the right part. This may be due even to a fabrication defect and also to a perspective effect (the inflatable beam does not remain exactly in an horizontal plane). It has been set constant (and found equal to 93.64 pixels on the picture). The perspective effect will be corrected soon.
- The ends, despite their description by an ellipse in order to take the perspective into account, are less well identified. Again, the composite ring which holds the inflatable beam may have been positioned with some imperfection and its color (gray) is not the best for correlation.
- Dark artifacts are due to some parasite reflexion (the image is inverted).
- The optical device yields a distorsion which should be taken into account soon.

This Euler-Bernouilli computation gives the final value (V_1 is divided by L to get a dimensionless number and avoid to convert pixels to meters) :

$$\frac{fL^3}{\left(E+\frac{P}{S}\right)I} = 1.16 \tag{8}$$

and the final distance $\Phi = 4.06\%$ ($B = 15$ pixels), however this value cannot be used alone as an indicator, as it depends on the arbitrary width B of the virtual image.
Secondly, the optimization takes into account the second term of Equation 4 (thus V_2 in Equation 7), related to Timoshenko theory and shear effects. The final result is (V_1 and V_2 are divided by L to get a dimensionless number and avoid to convert pixels to meters):

$$\frac{fL^3}{\left(E+\frac{P}{S}\right)I} = 0.634 \tag{9}$$

$$\frac{fL}{(P+kGS)} = 0.056 \tag{10}$$

the identified radius is 93.51 pixels on the picture (very close to the first measure) and the global error is $\Phi = 4.00\%$ ($B = 14$ pixels) which indicates a slightly better optimization than for the previous Euler-Bernoulli kinematics. The displacement obtained for the two kinematics of Euler-Bernoulli and Timoshenko are compared together on Figure 8. It shows that the Bernoulli approach underestimates a little the deflection. However this still does not constitute a sufficient argument in favor of the choice between the two models.

The mechanical properties in both Bernoulli and Timoshenko cases are deduced from these correlation results. The aerodynamical load is given by Equation 5, with a radius $R = 0.135$ m (which is the theoretical value), the average velocity is equal to $V = 20$ m/s, the volumetric mass density $\rho = 1.2$

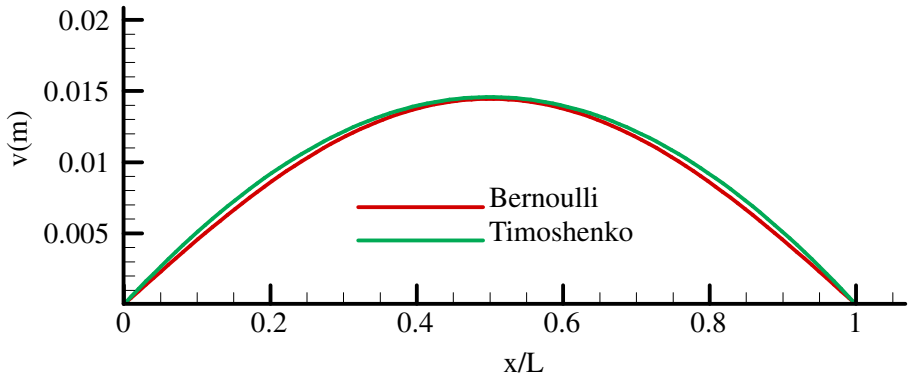

Figure 8 : Identified deflection of the beam under both Bernoulli and Timoshenko hypothesis.

kg/m^3 and the drag coefficient $C_x = 0.5$ (corresponding to the Reynolds number $Re = 3.5 \times 10^5$). Under those considerations, f is found equal to 32.4 N/m, leading to:

$$(Ee)_{Bernoulli} = 3.4 \times 10^5 \text{ N/m} \tag{11}$$

$$(Ee)_{Timoshenko} = 6.2 \times 10^5 \text{ N/m} \tag{12}$$

$$(Ge)_{Timoshenko} = 2.2 \times 10^3 \text{ N/m} \tag{13}$$

where e is the fabric thickness. The Young modulus from Timoshenko theory is nearly twice the Young modulus deduced from the Bernoulli theory. Therefore, the importance of Timoshenko hypothesis for inflatable beams is highlighted. Characterization tests have already been carried out on the Ferrari F302 [5] with $E = 2.2 \times 10^5$ N/m and $G = 5.2 \times 10^3$ N/m. These values appear to be rather different. However, the latter tests are fulfilled over a longer period than our measurements to consider creep effects. Moreover, the present test contains some remaining uncertainties:

- the beam does not stay in the horizontal plane
- there is some perspective effects acting on the radius and length values
- the loading is not absolutely uniform as expected by the model
- some gust of wind sometimes occur in the tunnel
- the inflating device suffers air leaks, leading to a ill-measured internal pressure (due to head losses in the air hose)

This test will be improved in the future. Force sensors will be installed on each cable. The knowledge of the inflation pression will be accurately determined by the use of a shorter inflation pipe (due to air leak, the beam is continuously inflated) and more accurate manometer fixed directly on the inflatable beam.

CONCLUSION

Methods of imagery such as VIC are able to measure the contour of a structure even if it is very deformable and large as it is the case for inflatable structures. The mentioned method has been presented in the context of lab-testing to validate design rules. Notwithstanding, the development of VIC in full SHM procedure appears to be quite easy and low cost; it only requires one camera (or at least two if 3D information are wanted) and it asks for reasonable computation power. Of course, in reality the night and the weather can sometime impeach or make the imaging process more difficult. But, considering a complete SHM procedure, it can provide the global displacement of a structure several times a day. This capital information should be of primary interest to determine the structure health state. Nethertheless, this protocole might be limited if the natural brightness varies along the day.

Compared to other edge detection methods (which are mostly used in medicine) the VIC provides a better precision. Contrarily, its lower detection capacity is not as crucial in the SHM field in which the structure generally keeps some fixed points such as the anchoring. The VIC method can also be joined to FEM computations [6]: this combination should be of great interest to perform SHM by the use of a stochastic model, including damage or plasticity.

REFERENCES

[1] F. Hild and S. Roux. Digital image correlation: from displacement measurement to identification of elastic properties-a review. *Strain*, 42, 2006.

[2] M. François, B. Semin, and H. Auradou. Identification of the shape of curvilinear beams and fibers. *Appl. Mech. and Mat.*, 24, 2010.

[3] B. Semin, H. Auradou, and M. François. Accurate measurement of curvilinear shapes by virtual image correlation. *Eur. Phys. J. Appl. Phys.*, 56, 2011.

[4] A. Le Van and C. Wielgosz. Bending and buckling of inflatable beams: some new theoretical results. *Thin-Walled Structures*, 43, 2005.

[5] Q.T. Nguyen. *Contribution à l'étude du gonflage, de la flexion, et du flambement de tubes membranaires orthotropes pressurisés*. PhD thesis, Ecole Centrale Nantes, 2013.

[6] J. Réthoré and M. François. Curve and boundaries measurement using B-splines and virtual images. *Optics and Lasers in Engng.*, 52, 2014.